TOTAL OZONE COLUMN DERIVED FROM GOME AND SCIAMACHY USING KNMI RETRIEVAL ALGORITHMS: VALIDATION AGAINST BREWER MEASUREMENTS AT THE IBERIAN PENINSULA

M. Antón[1], M. Kroon[2], M. López[3], J.M. Vilaplana[4], M. Bañón[3], R. van der A[2], J.P. Veefkind[2], P. Stammes[2] and L. Alados-Arboledas[1]

1. Departamento de Física Aplicada, Universidad de Granada, Granada, Spain
2. Department of Climate and Seismology, Royal Netherlands Meteorological Institute, PO-Box 201, NL-3730AE, De Bilt, Netherlands.
3. Departamento de Producción, Agencia Estatal de Meteorología, Madrid, Spain.
4. Departamento de la Tierra, Teledetección y Atmósfera, Estación de Sondeos Atmosférico El Arenosillo, INTA, Huelva, Spain.

Corresponding author: Manuel Antón, Departamento de Física Aplicada, Universidad de Granada, Granada, Spain.

Phone: +34 924 289536

Fax: +34 924 289651

e-mail: mananton@unex.es

ABSTRACT

This article focuses on the validation of the total ozone column (TOC) data set acquired by the Global Ozone Monitoring Experiment (GOME) and the SCanning Imaging Absorption spectrometer for Atmospheric CHartographY (SCIAMACHY) satellite remote sensing instruments using the TOGOMI and TOSOMI retrieval algorithms developed by the Royal Netherlands Meteorological Institute (KNMI). In this analysis, spatially co-located, daily averaged ground-based observations performed by five well-calibrated Brewer spectrophotometers at the Iberian Peninsula are used. The period of study runs from January 2004 to December 2009. The agreement between satellite and ground-based TOC data is excellent (R^2 higher than 0.94). Nevertheless, the TOC data derived from both satellite instruments underestimate the ground-based data. On average, this underestimation is 1.1% for GOME and 1.3% for SCIAMACHY. The SCIAMACHY-Brewer TOC differences show a significant solar zenith angle (SZA) dependence which causes a systematic seasonal dependence. By contrast, GOME-Brewer TOC differences show no significant SZA dependence and hence no seasonality although processed with exactly the same algorithm. The Satellite-Brewer TOC differences for the two satellite instruments show a clear and similar dependence on the viewing zenith angle (VZA) under cloudy conditions. In addition, both the GOME-Brewer and SCIAMACHY-Brewer TOC differences reveal a very similar behavior with respect to the satellite cloud properties, being cloud fraction and cloud top pressure, which originate from the same cloud algorithm (FRESCO+) in both the TOSOMI and TOGOMI retrieval algorithms.

1 INTRODUCTION

Upper tropospheric ozone plays a vital role in weather and climate on regional to global spatial scales when acting as a major greenhouse gas (Kiehl et al., 1999; Rex et al., 2004). In addition, the stratospheric ozone performs another vital function: That is to protect the biosphere from the most energetic part of the ultraviolet (UV) solar radiation spectrum. Therefore, close monitoring of the total ozone column has become a subject of major concern both by the scientific community and the general public.

Several studies have shown that there have been significant negative trends in stratospheric ozone abundances in the middle and high latitude regions of the two hemispheres since the end of the 1970s until the beginning of the 1990s [e.g., Stolarski et al., 1992; Callis et al., 1997; Solomon, 1999; Staehelin et al., 2001]. These negative trends have been associated with dynamical factors [Hood et al., 1997; Steinbrecht et al., 1998; Fusco and Salby, 1999; Appenzeller et al., 2000; Hadjinicolaou et al., 2002] and photochemical losses related to anthropogenic causes [Molina and Rowland, 1974; Farman et al., 1985; Stolarski et al., 1986, 1992; Bojkov et al., 1990; Harris et al., 1997]. The successful implementation of the Montreal Protocol and its Amendments has halted the increase of substances that deplete the stratospheric ozone layer. Scientists now see the first signs of a reduction of ozone-depleting substances which has created high expectations about the recovery of the global ozone layer towards pre-1980s amounts [World Meteorological Organization (WMO), 2010] in the second half of the 21st century.

Remote sensing instruments operating on satellite platforms offer the most effective vantage point to monitor the global ozone layer by accurately deriving the geographical and temporal distribution and variability of the total ozone column (TOC) from measurements of backscattered solar UV radiation [McPeters et al., 1998; Bovensmann et al., 1999; Burrows et al., 1999; Levelt et al., 2006; Munro et al., 2006]. These satellite observations have proven to be crucial for accurately assessing the current state of the global ozone layer and to foster trustworthy predictions of its future changes. Satellite TOC data complement ground-based observations, providing daily images of the global ozone distribution with good spatial resolution. Within this framework, the two European satellite-borne atmospheric sensors named GOME (Global Ozone Monitoring Experiment) [Burrows et al., 1999] and SCIAMACHY (SCanning Imaging Absorption spectrometer for Atmospheric CHartographY) [Bovensmann et al., 1999] provide an outstanding global ozone data record. While SCIAMACHY is currently operational and in good health, GOME has unfortunately been switched off in July 2011, offering the potential for an assessment of the global TOC distribution covering a time span of over 16 years

The accuracy of the TOC data currently retrieved from the observations by satellite instruments covering the ultraviolet (UV) spectral range is, in general, very high as they compare to well-established ground-truth reference data within a few percent [Fioletov et al., 2002; Bramstedt et al., 2003; Balis et al., 2007a; 2007b; Lerot et al., 2009; Antón et al., 2010a; Loyola et al, 2011]. To assure these high-quality observations and to clarify local to regional specific sources of uncertainties, validation exercises on a regular basis against accurate and independent measurements inferred from reference ground-based instruments are required. For instance, the Spanish Network of Brewer spectrophotometers consists of five well-calibrated and well-maintained instruments located on the Iberian Peninsula. These instruments follow exactly the same protocol of calibration and in this way the ozone calibration of all Spanish Brewer spectrophotometers is traceable to the triad of international reference Brewers maintained by Environment Canada (EC) at Toronto [Fioletov et al., 2005]. The main advantage of using a dense local ground-based network for validation purposes is that all instruments involved measure the same atmospheric quantity at the same time and at nearly the same location which further improves their correspondence. This regional network has been successfully used to perform exhaustive validation exercises on satellite TOC data derived from instruments onboard several satellite platforms [Antón et al., 2008; 2009a; 2009b; 2010a; 2010b; 2011]. The TOC data recorded by the Spanish Brewer Network have also been successfully used to analyze the influence of clouds on the

TOC observations provided by several UV-type satellite instruments [Antón and Loyola, 2011].

The main objective of this work is to validate the TOC data derived from the observations by the GOME and SCIAMACHY instruments using as a reference the spatially and temporally collocated ground-based observations from five Brewer spectrophotometers in the Iberian Peninsula. TOC data recorded between January 2004 and December 2009 are used for this satellite-ground-based inter-comparison. In this work, the satellite TOC data inferred from the retrieval algorithms developed by the Royal Netherlands Meteorological Institute (KNMI) which employ the by now standard Differential Optical Absorption Spectroscopy (DOAS) technique [e.g., Solomon et al., 1987; Platt, 1994, 1999] are used. These two retrieval algorithms are the Total Ozone retrieval scheme for the GOME instrument based on the Ozone Monitoring Instrument DOAS algorithm (TOGOMI) [Valks and van Oss, 2003], and the corresponding application to the SCIAMACHY instrument (TOSOMI) [Eskes et al., 2006]. Although global-scale validation exercises of GOME and SCIAMACHY TOC data derived from the KNMI algorithms have been independently performed before [e.g., Balis et al., 2003; van Oss et al., 2004; Eskes et al., 2005; 2006], the present work should be considered to be complementary since a simultaneous validation of the two KNMI algorithms using the same reference ground-based instruments and with a focus on the influence of cloud properties has not yet been performed in detail. Furthermore, in this paper the latest version of both algorithms is used which has not been analyzed before. It is therefore expected that this paper will contribute to improving the understanding of the quality of the GOME and SCIAMACHY TOC observations retrieved by the KNMI algorithms.

The ground-based instrumentation and the satellite data used in this paper are described in section 2. Section 3 describes the methodology of the analysis. Section 4 presents and discusses the results obtained and, finally, section 5 summarizes the main conclusions drawn from this work.

2 TOTAL OZONE COLUMN DATA

2.1 Satellite observations

The ESA GOME instrument is an across-track scanning nadir-viewing UV-VIS spectrometer on board the Second European Remote Sensing Satellite (ERS-2) [Burrows et al., 1999]. GOME has been recording global TOC observations from July 1995 until June 2003, when due to the failure of the tape recorder of ERS-2 the data coverage of GOME became limited to the north hemispheric receiving stations of ESA. Nevertheless, the Iberian Peninsula has been continuously covered by GOME from July 1995 until the instrument was switched off in July 2011. Nominally, global coverage at the Equator is achieved by GOME within three days. The ground swath (960 km) is divided into three ground pixels of 320 km (across orbit) × 40 km (along orbit). The SCIAMACHY instrument is a joint German–Dutch–Belgian contribution to the ESA ENVIronmental SATellite (ENVISAT) platform which was launched in March 2002 [Bovensmann et al., 1999]. This satellite instrument records atmospheric spectra from alternating nadir and limb viewing geometries, and in addition, provides measurements from solar and lunar occultation modes. In this work, only data derived from nadir mode have been used. SCIAMACHY has a total swath width of 960 km with a typical spatial resolution in nadir of 60 km across track by 30 km along track and it achieves global coverage in approximately six days at the equator because of the additional limb observations.

The retrieval of TOC data from these two European satellite instruments is performed by three different DOAS-type retrieval algorithms: GDOAS/SDOAS developed from BIRA-IASB and DLR [van Roozendael et al., 2006; Lerot et al., 2009], GOME-WFDOAS/SCIA-WFDOAS from University of Bremen [Coldewey-Egbers et al., 2004; Bracher et al., 2005] and TOGOMI/TOSOMI from KNMI [Valks and van Oss, 2003; Eskes et al., 2006]. TOGOMI (version 2.0) and TOSOMI (version 2.0) are the retrieval algorithms used in this work for deriving TOC data from the observations by GOME and SCIAMACHY, respectively. These two algorithms are based on the DOAS method developed by KNMI for the Ozone Monitoring Instrument (hereafter denoted as

OMI-DOAS) [Veefkind et al., 2006]. The differences between the TOGOMI and TOSOMI retrieval algorithms are only on the programming level (e.g., different level-1B reading routines). Thus, the main characteristics of TOGOMI/TOSOMI algorithms (version 2.0) are:

1. The use of the BDM (Brion, Daumont, Malicet) ozone absorption cross-section.

2. The use of a semi-spherical polarization-dependent radiative transfer model for the simulations of spectra and, consequently, for the calculation of the air mass factor (AMF) [De Haan, 1987].

3. AMF computation as a function of Sun-satellite geometry, surface reflectivity, surface pressures and ozone profile using an empirical approach [Marquard et al., 2000].

4. The ozone profiles are taken from TOMS version 8 ozone profile climatology [Bhartia and Wellemeyer, 2002].

5. Treatment of the atmospheric temperature sensitivity by using effective ozone cross-sections calculated from ECMWF temperature profiles.

6. The Fast Retrieval Scheme for Clouds from the Oxygen A-band (FRESCO+) algorithm (version 6) is used for the treatment of clouds [Wang et al., 2008]. In FRESCO+, the cloud top albedo is assumed to have a fixed value of 0.8, and the so-called “effective” cloud top pressure (CTP) and “effective” cloud fraction (CF) are fitted using reflectances around the Oxygen A-band. The version 6 of FRESCO+ algorithm uses the new MERIS surface albedo climatology in the Oxygen A-band over land [Popp et al., 2011], and over ocean the GOME surface albedo climatology, and the HITRAN 2008 database of molecular spectroscopy, which were not yet incorporated in the previous versions of FRESCO+ algorithm.

7. A new treatment of Raman scattering in DOAS which explicitly accounts for the Raman smoothing of the solar Fraunhofer lines as well as the ozone absorption structures [De Haan, 2003].

The TOGOMI/TOSOMI version 2.0 algorithms replace the previous versions (1.3 for TOGOMI and 0.43 for TOSOMI) and they are improved with respect to the interpolation of the surface reflectivity and the use of the latest version of the FRESCO+ cloud algorithm (version 6). SCIAMACHY level-1B data is of version 7 and GOME level-1B data is of version 4. TOGOMI and TOSOMI TOC data are distributed via internet through the Tropospheric Emission Monitoring Internet Service (TEMIS) which can be found at http://www.temis.nl .

2.2 Ground-based measurements

The Spanish Brewer Network consists of five Brewer spectrophotometers at the Iberian Peninsula located from North to South at: A Coruña (43.33ºN, 8.42ºW), Zaragoza (41.01ºN, 1.01ºW), Madrid (40.45ºN, 3.72ºW), Murcia (38.03ºN, 1.17ºW) and El Arenosillo (37.06ºN, 6.44ºW). All Brewer instruments are type MK-IV (single monocromator), except the Brewer MK-III (double monocromator) located at El Arenosillo. Figure 1 shows the distribution of these five Brewer locations over the Iberian Peninsula. This dense local network is managed by the Spanish Agency of Meteorology (AEMET) which has accumulated nearly twenty years of experience in measuring TOC data with Brewer spectrophotometers. The Spanish Brewer Network possesses an excellent maintenance record since all spectrophotometers are biannually calibrated by inter-comparison with travelling references Brewer 017 from International Ozone Services (IOS) and Brewer 185 from the Regional Brewer Calibration Centre-Europe (RBCC-E). Comparisons between these two traveling reference instruments confirm the reliability of the Spanish Brewer calibration [Redondas et al., 2002; 2008].

The Brewer instruments rely on the method of differential absorption in the Huggins band of the ultraviolet spectral region where solar radiation experiences a strong absorption by atmospheric ozone. TOC data are obtained by taking the ratio of sunlight intensities at four wavelengths between 306 and 320 nm with a resolution of 0.6 nm, and by using the Bass and Paur (BP) ozone absorption cross-sections at a fixed temperature of −45ºC [Kerr, 2002]. Literature shows that Brewer systems yield near similar results when its operational retrieval is being performed with either the BDM or BP ozone absorption cross section data set [Redondas and Cede, 2006]. These authors have also shown that with either cross section data sets there is little to no dependence of the Brewer TOC estimate on the atmospheric temperature at which the ozone resides. When Brewer spectrophotometers are properly calibrated and regularly maintained, as is the case for the entire Spanish Brewer Network, the TOC records obtained through the direct sunlight (DS) measurements have the potential to maintain a precision of 1% over long periods of time [WMO, 1996].

3 METHODOLOGY

The Brewer TOC data used in this work are obtained from direct sun (DS) measurements only which are exclusively measured under cloud-free conditions during the day. Here cloud-free means those observations that are preceded and followed by truly cloud free observations over a time span of 3 minutes while the Brewer instrument records direct sunlight. In contrast, the satellite takes the corresponding punctual observation under any sky condition. In our analysis we differentiate between three different sky conditions: cloud-free, broken-cloud and fully clouded. The "effective" cloud fraction derived from the FRESCO+ algorithm is used to make this distinction where satellite ground pixels with a cloud fraction (CF) smaller than 5% correspond to cloud-free conditions, those with a CF higher than 50% are related to fully clouded conditions, and the cases with the CF between 5% and 50% are associated with broken-cloud conditions.

For inter-comparison purposes, the several Brewer measurements performed each day are averaged. The use of daily averaged ground-based TOC data instead of, for example, hourly averaged data centered on the satellite overpass provides a significant increase of the number of satellite-Brewer data pairs in the analysis as there is less interference by clouds on the Brewer observations. Over the Iberian Peninsula the ozone layer is largely dominated by the stratospheric contribution which is assumed to be stable during daytime, owing to the well-known long-term chemical stability of stratospheric ozone over middle latitudes.

In this work, the satellite pixel most closely collocated with the ground-based stations is selected as the best match everyday. The SCIAMACHY overpass is selected such that the distance between the center of the satellite pixel and the location of the ground-based stations is always less than 100 km while the GOME overpass is selected for a distance less than 200 km. This large difference in the spatial collocation criteria is related to the different satellite footprint ground pixel size of the two instruments: 60 x 30 km^2 (SCIAMACHY) and 320 x 40 km^2 (GOME).

The relative differences (RD) between the daily Brewer (Bre) TOC data and the satellite

TOC data (Sat) were calculated for each ground-based station using the following expression:

$$RD_i = 100 \times \frac{Sat_i - Bre_i}{Bre_i} \qquad (1)$$

From these relative differences, the mean bias (MB) and the mean absolute bias (MAB) parameters were also calculated as:

$$MB = \frac{1}{N}\sum_{i=1}^{N} RD_i \qquad (2)$$

$$MAB = \frac{1}{N}\sum_{i=1}^{N} \left|RD_i\right| \qquad (3)$$

where N is the number of data pairs Satellite-Brewer recorded in each ground-based station. While the MB parameter shows the degree of underestimation or overestimation of the TOC data derived from satellite instruments with respect to the reference Brewer measurements, the MAB parameter reports about the absolute value of the relative differences between satellite and ground-based data.

Time series of both satellite and ground-based TOC data extend from January 2004 to December 2009. Table 1 shows the number of pairs of ground-based-satellite data used in this work. In addition, a linear regression analysis is performed between the TOC values recorded by the Brewer spectrophotometers and the two satellite instruments. Regression coefficients, coefficients of correlation (R^2) and the root mean square errors (RMSE) are evaluated in this analysis.

4 RESULTS AND DISCUSSION

4.1 Regression analysis

Firstly, a linear regression analysis between the ground-based Brewer TOC data and the satellite-based TOC data derived from GOME and SCIAMACHY observations is performed in order to analyze their proportionality and similarity. Statistical parameters obtained from the linear fitting between satellite-based and ground-based data are shown in Table 1 for the five ground-based stations and for the "Iberian Peninsula" dataset (all data). The correlation between the satellite-based and ground-based TOC data is significantly high for both satellite instruments with correlation coefficients higher than 0.94 for all cases. In addition, the statistical analysis renders slopes very close to unity, indicative of their proportionality. The two scatter plots shown in Figure 2 between satellite-based and ground-based TOC data reveal this high degree of agreement. The solid line is the unit slope line with zero bias. The minus sign of the MB parameters for the two correlations indicate that both GOME and SCIAMACHY TOC data underestimate the Brewer data. On average, the underestimation is 1.08% with ± 2.29% one standard deviation for GOME and (1.26 ± 2.25)% for SCIAMACHY. A value of the standard deviation smaller than 3% suggests that the random and systematic errors of TOC data inferred from both satellite instruments are relatively small. Our results are in accordance with global validation exercises of TOGOMI/TOSOMI retrieval algorithms. For instance, Eskes et al. [2005] reported that TOSOMI TOC data (version 0.32) have an offset of about (–1.7 ± 4.4)% with respect to ground-based observations. Balis et al. [2003] indicated that the satellite TOC data from TOGOMI are on the average slightly lower (~0.5%) than the ground-based ones.

Table 1 shows that for the two satellite instruments, the MB and MAB parameters have similar absolute values. This fact reveals the presence of a significant bias in the satellite data with respect to the reference ground-based measurements. Thus, the MAB parameter present a value of (1.90 ± 1.68)% for GOME, and (1.99± 1.63)% for SCIAMACHY. Additionally, the statistical parameters obtained for each ground-based station are compared with each others since the surface albedo may affect the TOC data derived from satellite instruments. The surface albedo comes into play via the cloud fraction and cloud top height estimates, which are used to correct for the tropospheric ghost column that the clouds are hiding from the satellite instrument to see. These cloud parameters are obtained from the visible spectral range of the satellite instruments where the radiance is sensitive to the surface albedo. Thus, for instance, at coastal stations, the nearby sea (which has a low albedo) could affect the ozone retrieval, since the satellite ground pixel may be filled with part land and part ocean scene. Table 1 shows that the statistical parameters for inland and coastal Brewer stations (see Figure 1) are similar. For example, the difference between the maximum MAB value (2.23% at Coruña) and the minimum (1.49% at El Arenosillo) for the GOME-Brewer analysis is only 0.74% while for the SCIAMACHY-Brewer analysis, the difference between the maximum MAB value (2.52% at Murcia) and the minimum (1.57% at El Arenosillo) is 0.95%. These small values for the station-to-station biases indicate that the locations of the five Brewer stations present no significant influence on the satellite - ground-based differences. This result underlines both the consistency and high reliability of the Spanish Brewer Network and the success in the correction of the albedo effects by the satellite retrievals.

4.2 Temporal evolution of the satellite - ground-based differences

It is interesting to analyze the temporal evolution of the daily relative differences between ground-based and satellite-based TOC data. The daily relative difference for a specific day is obtained as the mean value of all relative differences for each day (a maximum of five values per day from the five ground-based stations). The time series of the ten-day running average of the daily mean relative differences for the period 2004–2009 is shown in the two plots of Figure 3. A slight seasonal dependence can be seen in the relative differences between SCIAMACHY TOC data and the Brewer TOC data for the entire period of comparison with the largest differences occurring in the summer. In contrast, Figure 3 (bottom) does not reveal any seasonality for GOME-Brewer differences, showing a remarkably constant behavior over the period of comparison. This result is in agreement with the global validation results of TOGOMI data given by Balis et al. [2003] that also showed no significant seasonal variability over most of the northern hemisphere. The relative differences between SCIAMACHY and Brewer TOC data (equation 1) present values within ±1%, ±3% and ±5% for 34%, 82% and 97% of all days, respectively. For GOME–Brewer relative differences, the percentages increase to 38%, 87% and 98%, respectively. These results indicate that the general bias is slightly less for GOME than for SCIAMACHY instrument. Furthermore, there is no evidence for significant change in the GOME and SCIAMACHY TOC data over the period of comparison despite the regular decontaminations of the SCIAMACHY instrument and the unavoidable optical and detector performance degradation over the course of the satellite instrument lifetimes.

4.3 Dependence of the differences on geometrical parameters

The seasonal dependence presented in Figure 3 (top) for SCIAMACHY suggests that its TOC observations may depend on the ground pixel solar zenith angle (SZA). Using 5º bins of SZA, Figure 4 (top) shows the mean relative differences between ground-based and satellite TOC data as a function of satellite ground pixel SZA for SCIAMACHY. The SZA dependence has been analyzed using four datasets: all data (in black), cloud-free cases (CF<5%, in red), fully clouded condition (CF>50%, in blue), and broken-cloud cases (5%<CF<50%, in pink), with CF being the "effective" cloud fraction derived from FRESCO+ algorithm as explained in section 2.1. The percentage of cases selected is about 33% for cloud-free conditions, 14% for fully clouded conditions, and 53% for broken-cloud conditions. Error bars represent the standard errors which are only plotted for cloud-free and fully clouded conditions, in the interest of clarity. The curves corresponding to all sky conditions, fully clouded conditions and broken-cloud cases follow a similar pattern, showing a monotonic decrease in underestimation as a function of satellite SZA. Nevertheless, the SCIAMACHY–Brewer relative differences under fully clouded and broken-cloud conditions reveal a higher amplitude in their SZA dependence (from -2% to +1%, and from -2.5% to -0.5%, respectively) than the differences for all sky cases (from -2% to -0.5%). By contrast, the curve associated with cloud-free conditions shows a more stable behaviour for the whole range of SZA. It can be seen that for SZA values up to 50º, the underestimation is always smaller for both cloud-free and cloudy cases than for broken-cloud conditions. In addition, for these angles up to 50º, the curve associated with fully clouded cases shows no significant dependence on SZA, with values between -1% and -2%. Nevertheless, this curve shows a large jump around the satellite SZA of 45º-50º. Thus, the satellite to ground-based differences under fully clouded cases present values close to 0% for SZA values higher than 50º (except the last bin where the relative difference increases to 1%). All these results indicate that the SZA dependence observed for SCIAMACHY TOC data could be related to sky conditions in terms of cloud fraction. This result is in agreement with the work of Antón and Loyola [2011] which showed that the SCIAMACHY TOC data derived from the SDOAS prototype algorithm developed by BIRA-IASB and DLR presented no significant dependence on SZA for cloud-free cases, while showing a clear SZA dependence during cloudy conditions for angles higher than 50º, but not for smaller angles. In addition, these authors also showed that the satellite-Brewer differences obtained with the OMI-DOAS algorithm, which formed the early basis for the TOGOMI/TOSOMI algorithms, have a large dependence on SZA for cloudy cases only. This SZA dependence under cloudy cases was explained by the fact that the effects of the presence of clouds in the scene on the ozone retrieval decreases with increasing SZA since at high SZA the radiative transfer is dominated by scattering-absorption processes in the stratosphere rather than the scattering-absorption processes occurring in the troposphere which contribute more to the slant column for low SZA [Koelemeijer and Stammes, 1999].

Figure 4 (bottom) shows the mean relative differences between Brewer data and GOME data as a function of satellite ground pixel SZA for the four datasets corresponding to all, cloud-free (CF<5%), fully clouded conditions (CF>50%), and broken-cloud cases (5%<CF<50%). It is noted that for the GOME data set, 26% of the cases are for cloud-free conditions, 13% are for fully clouded conditions and 61% for broken-cloud cases. The curves associated with all, cloud-free and broken-cloud cases show practically no dependence on the GOME SZA over the Iberian Peninsula, in agreement with and confirming the null-seasonal behavior shown in Figure 3 (bottom) using all data. The curve corresponding to fully clouded cases also presents a constant negative bias around -1.5% for SZA smaller than 45º, showing at this SZA a large jump. Thus, the satellite to ground-based differences for the fully clouded conditions are between -1% and +0.5% for SZA higher than 45º. Therefore, the SZA dependence observed in SCIAMACHY, but not in GOME, almost certainly is not related to problems in the retrieval algorithm, since the TOSOMI and TOGOMI algorithms used in this work to retrieve TOC data from SCIAMACHY and GOME are practically identical. This SZA dependence (and seasonality) found for SCIAMACHY data could be due to inaccuracies in the level 0 (raw data) to level-1B (calibrated radiances) processing. In this sense, despite substantial efforts to improve the radiometric calibration of SCIAMACHY regarding polarization effects, spectral effects and the reanalysis of pre-flight calibration data [e.g., Tilstra and Stammes, 2005; Skupin et al., 2005; Gurlit et al., 2005], there are still uncertainties about the radiometric calibration of SCIAMACHY in the UV.

Another outstanding parameter that describes the viewing geometry of the satellite observations is the viewing zenith angle (VZA) of the satellite ground pixel. The SCIAMACHY instrument measures 16 scenes along the ground swath, one for each satellite VZA stepping at 5° intervals between −40° and +40. By contrast, the GOME instrument has only three scan positions between a VZA of −30° and +30°. Thus, it is very interesting to analyze whether the variation of the satellite VZA affects the differences between satellite and ground-based TOC data. Figure 5 shows two plots where the Satellite-Brewer relative TOC differences are plotted as a function of the satellite VZA for SCIAMACHY (top) and GOME (bottom). Four curves are shown in each plot corresponding to all cases, cloud-free conditions, fully clouded conditions, and broken-cloud cases. For the SCIAMACHY instrument, the satellite to ground-based difference under cloud-free conditions shows a slight dependence on satellite VZA, varying from -1.2% for the outermost east pixels (negative scan angles) to -0.3% for the outermost west pixels (positive scan angles). On the other hand, the SCIAMACHY TOC data corresponding to all sky conditions, fully clouded conditions and broken-cloud cases present for west pixels a greater underestimation with respect to Brewer data than for east pixels. In addition, there is a clear difference between the curve corresponding to cloud-free conditions and the other curves for west pixels. Similar results were shown by Antón and Loyola (2011) for the SCIAMACHY TOC data derived from the SDOAS prototype algorithm in which the FRESCO+ cloud parameters are ingested off-line by running the FRESCO+ algorithm. Figure 5 (bottom) shows a significant variation between the GOME-Brewer relative difference obtained during fully clouded conditions for the east scene (+0.4%) and the difference for the west scene (-1.7%). In contrast, for cloud-free conditions, the variations of the relative differences between the east and the west scene are significantly smaller. Therefore, the notable influence of VZA on the Satellite-Brewer differences under cloudy conditions for both SCIAMACHY and GOME could be related to sky conditions in terms of effective cloud fraction and cloud top pressure derived by the FRESCO+ algorithm.

If polarization, or a polarization calibration issue, would be the reason that the SZA dependence of the Total Ozone Column Differences (DTOC) is much stronger for SCIAMACHY than for GOME, the scattering angle should be used as an x-value or parameter. The reason is that polarization of atmospheric radiation depends on the scattering angle, that is the angle between incident sunlight and reflected light towards the satellite. Some information on the DTOC as a function of the scattering angle is presented in Figure 5. Furthermore, Figure 5 shows that the dependence of the DTOC on VZA for SCIAMACHY and GOME is of the same order of magnitude. The east viewing directions have a scattering angle closer to 90 degrees than the west viewing directions. This causes the Rayleigh scattered sunlight received in the east viewing directions to be more strongly polarized than the west viewing directions. In case of a strong polarization dependent sensitivity of SCIAMACHY and GOME, an East-West difference in DTOC should appear most clearly for the cloud free scenes when Rayleigh scattering dominates the received signal. In the case of cloudy scenes, the light scattered by clouds is depolarized and will dominate the scene brightness hence a dependence on VZA of DTOC is then not expected. However, our analysis shows that the opposite situation is the case hence a polarization dependent sensitivity of SCIAMACHY or GOME does not seem to play a role.

4.4 Dependence of the differences on cloud parameters

Under cloudy conditions, the accurate determination of the effective cloud fraction and the effective cloud-top pressure by the satellite retrieval algorithm plays an important role in two respects: (1) the calculation of the air mass factor (AMF) which makes the conversion from the ozone slant column to the vertical column density, and (2) the estimation of the ozone amount below the effective cloud top, labeled the ghost column, since the satellite is only sensitive to the ozone concentration above the effective cloud top. Thus, it is interesting to analyze the influence of the cloud properties (effective cloud fraction and effective cloud-top pressure) in the satellite-ground-based difference.

The relative differences as a function of cloud fraction (using bins of 10%) as reported by SCIAMACHY (top) and GOME (bottom) are shown in Figure 6. Each plot shows three curves corresponding to all (in black), low (in red) and high (in blue) SZA values. Error bars (standard error) are plotted for the curves related to low and high SZA. It can be seen that SCIAMACHY (Figure 6, top) shows large biases between the similar curves corresponding to low and high SZA cases for all sky conditions. Thus, the TOC data inferred from this satellite instrument for small SZA values clearly show a larger underestimation of the ground-based data than the TOC data for high SZA values while its dependence on cloud fraction is similar. In contrast, the GOME data (Figure 6, bottom) shows a more homogeneous pattern for the three curves. Nevertheless, the wave-like evolution of the relative differences as function of CF is very similar for the two satellite instruments. This behavior is in accordance with the two satellite algorithms using the same algorithm for the treatment of clouds (FRESCO+). Thus, the underestimation of Brewer data by SCIAMACHY and GOME data slightly increases from cloud-free conditions until partially cloudy cases (CF between 10% and 20%). For instance, the SCIAMACHY relative differences using all data vary from (-1.1±0.1)% (0%<CF<5%) to (-1.8±0.1)% (20%<CF<30%). Then, there is a reversal of this negative bias, thus the underestimation shows a significant decrease until CF ≈75%. Following the example, the SCIAMACHY relative differences using all data present a value of -0.1% for the CF interval between 70% and 80%. Finally, a second negative trend appears for fully clouded cases, where the SCIAMACHY differences reach values of -1.4% for the CF interval between 90% and 100%. A similar evolution of the SCIAMACHY-Brewer differences as a function of CF was shown by Antón and Loyola [2011]. These authors worked with SCIAMACHY TOC data derived from the SDOAS prototype algorithm using the FRESCO+ algorithm. Therefore, this cloud algorithm could very well be the main culprit for the behavior shown in Figure 6 for both SCIAMACHY and GOME data.

Figure 7 shows the dependency of the satellite-ground-based relative differences with respect to the satellite cloud-top pressure (CTP) for all, low and high SZA values. The CTP values are derived from the fitting of the reflectances around the Oxygen A-band as was explained in the subsection 2.1. This analysis was performed where CF >5%. It can be seen that the behavior with CTP is very similar for the two satellite instruments but with larger biases between the curves corresponding to low and high SZA cases for SCIAMACHY and a smoother behavior for GOME in accordance with Figure 6. The relative differences show a marked negative dependence with respect to the CTP. For SCIAMACHY, a slight overestimation (~ 1%) can be seen for high clouds (CTP between 200 mb and 300 mb) when all data are used (black curve). A similar pattern of overestimation of ground-based TOC data was found for the OMI-DOAS algorithm by Antón and Loyola [2011] who suggested that it could be related to the underestimation of the cloud-top pressure for high clouds and the consequently overestimated “ghost” column added to the retrieved above-cloud column amount for these cases. In addition, the two plots in Figure 7 show a clear underestimation for the curves corresponding to all and small SZA under the lowest clouds (CTP between 900 mb and 1000 mb). This underestimation is stronger for SCIAMACHY than for

GOME, although the bias of both instruments is similar for the curve associated with high SZA. Thus, this issue seems to originate from the SZA dependence and not from the CTP itself. Other possible explanation could be in the different percentage of cloudy cases (CF>5%) with CTP values higher than 900 mb found for the two satellite instruments. While SCIAMACHY presents about 17% of all cloudy cases with CTP values higher than 900 mb, GOME has about 9% of these cases. Antón and Loyola [2011] reported that many of the SCIAMACHY cases classified as low clouds really correspond to cloud-free observations.

4.5 Dependence of the differences on ground-based TOC data

Finally, the relative differences between ground-based and satellite TOC data as a function of the Brewer TOC data (using bins of 20 DU) are analyzed in Figure 8 (top, SCIAMACHY; bottom, GOME) for all, low and high SZA values. The SCIAMACHY relative differences show a negative dependence with TOC between 240 and 320 DU when all SZA conditions are used in the analysis. Here the relative differences vary from 0% (240 DU) to -1.8% (320 DU). For the rest of ground-based TOC values, the SCIAMACHY data show a constant underestimation of the Brewer data. The blue and red curves corresponding to low and high SZA values show a very different behavior. While the blue curve has an almost smooth negative dependence on ground-based TOC, the red curve reveals a constant negative bias around -2%. This result is in accordance with the temporal evolution showed in Figure 3 (top), where the SCIAMACHY data underestimate the TOC by -2% to -3 for the months between May and September. On the other hand, Figure 8 (bottom) also shows that the three datasets of GOME relative differences have a clear dependence with respect to ground-based data for a broad range of TOC values. For instance, the relative differences change from -0.5% (250 DU) to -2% (400 DU). These results are in agreement with the GOME TOC data derived from the GDOAS algorithm developed by BIRA-IASB and DLR [Antón et al., 2008; 2009]. The near-linear dependence on ground-based TOC found for SCIAMACHY (between 240 DU and 320 DU) and GOME (between 250 DU and 400 DU) can be associated with the

SZA/seasonal dependence explained in subsections 4.2 and 4.3.

5 CONCLUSIONS

The main conclusion drawn from this validation exercise is that the SCIAMACHY TOC data derived by the TOSOMI algorithm present a significant SZA dependence which produces a systematic seasonal dependence with respect to reference ground-based TOC observations. This behavior is not found for the GOME data inferred from TOGOMI algorithm using the same well-calibrated ground-based spectrophotometers and the same period of study (2004-2009). TOSOMI and TOGOMI retrieval algorithms are identical with differences only in the level-1B reading routines. Therefore, the strong SZA dependence observed for TOSOMI data being absent in TOGOMI data should be mainly associated with instrumental differences in terms of calibration issues which then propagate into the level-1B (calibrated radiances) data of SCIAMACHY.

The Satellite-ground-based relative differences reveal a significant dependence on satellite VZA under cloudy conditions for both SCIAMACHY and GOME instruments. In contrast, the relative differences for cloud-free cases show a near constant behavior, suggesting that the dependence found for cloudy cases should be associated with the ingested cloud properties originating from the FRESCO+ by algorithm for the TOSOMI and TOGOMI algorithms

This work has also shown that for both GOME and SCIAMACHY the satellite-ground-based differences present a rather similar behaviour with respect to satellite pixel cloud properties (effective cloud fraction and effective cloud top pressure). This similarity is due to the cloud information given by the FRESCO+ code used in the two retrieval algorithms. Nevertheless, it should be underlined that GOME TOC data present a smoother behavior than SCIAMACHY TOC data which could be related to the issues commented above.

Finally, the satellite-ground-based relative differences show a negative dependence on total ozone for SCIAMACHY (between 240 DU and 320 DU) and for GOME (between 250 DU and 400 DU) which may be related the SZA/seasonal dependence.

This study leads us to conclude that despite these observations, which all fall within the ±5%

range, the TOSOMI/TOGOMI algorithms from KNMI provide a total ozone data set of great quality which is highly suitable for global ozone column monitoring.

The conclusions drawn from this work should only be considered as representative for the area of study. All results are based on five ground-based instruments located on the Iberian Peninsula, and hence this validation exercise should be seen as complimentary to global scale validation studies.

ACKNOWLEDGMENTS

The authors would like to thank the teams responsible for the provision of satellite and ground-based data used in this paper: the GOME and SCIAMACHY data derived from TOGOMI/TOSOMI algorithm were generated by the TEMIS service (www.temis.nl) hosted by the Royal Netherlands Meteorological Institute (KNMI); The Brewer ozone data used in this study have been provided by the Spanish Agency of Meteorology (AEMET) (Madrid, Murcia, Zaragoza and A Coruña) and the Spanish Institute of Aerospace Technique (INTA) (El Arenosillo). Manuel Anton thanks the Ministerio de Ciencia e Innovación and Fondo Social Europeo for the award of a postdoctoral grant (for Juan de la Cierva). This work was partially supported by the Andalusian Regional Government through projects P08-RNM-3568 and P10-RNM-6299, the Spanish Ministry of Science and Technology through projects CGL2010-18782 and CSD2007-00067, and by European Union through ACTRIS project (EU INFRA-2010-1.1.16-262254).

REFERENCES

Antón M., D. Loyola, B. Navascúes, and P. Valks (2008), Comparison of GOME total ozone data with ground data from the Spanish Brewer spectroradiometers, Ann. Geophys., 26, 401–412, doi:10.5194/angeo-26-401-2008.

Antón M., D. Loyola, M. López, J. M. Vilaplana, M. Bañón, W. Zimmer, and A. Serrano (2009a), Comparison of GOME-2/MetOp total ozone data with Brewer spectroradiometer data over the Iberian Peninsula, Ann. Geophys., 27, 1377–1386, doi:10.5194/angeo-27-1377-2009.

Antón M., M. López, J. M. Vilaplana, M. Kroon, R. McPeters, M. Bañón, and A. Serrano (2009b), Validation of OMI-TOMS and OMI-DOAS total ozone column using five Brewer spectroradiometers at the Iberian peninsula, J. Geophys. Res., 114, D14307, doi:10.1029/2009JD012003.

Antón, M., M. E. Koukouli, M. Kroon, R. D. McPeters, G. J. Labow, D. Balis, and A. Serrano (2010a), Global validation of empirically corrected EP-Total Ozone Mapping Spectrometer (TOMS) total ozone columns using Brewer and Dobson ground-based measurements, J. Geophys. Res., 115, D19305, doi:10.1029/2010JD014178.

Antón M., J. M. Vilaplana, M. Kroon, A. Serrano, M. Parias, M. L Cancillo, and B. de la Morena (2010b), The empirically corrected EP-TOMS total ozone data against Brewer measurements at El Arenosillo (Southwestern Spain), IEEE Trans. Geosci. Remote Sensing, 48, 3039-3045, doi: 10.1109/TGRS.2010.2043257.

Antón, M., D. Loyola, C. Clerbaux, M. López, J. M. Vilaplana, M. Bañón, J. Hadji-Lazaro, P. Valks, N. Hao, W. Zimmer, P. F. Coheur, D. Hurtmans, and L. Alados-Arboledas (2011), Validation of the METOP-A total ozone data from GOME-2 and IASI using reference ground-based measurements at the Iberian Peninsula, Rem. Sen. Environ., 115, 1380–1386, doi:10.1016/j.rse.2011.01.018.

Antón, M., and D. Loyola (2011), Influence of cloud properties on satellite total ozone observations, J. Geophys. Res., 116, D03208, doi:10.1029/2010JD014780.

Appenzeller, C., A. K. Weiss, and J. Staehelin (2000), North Atlantic Oscillation modulates total ozone winter trends, Geophys. Res. Lett., 27, 1131–1134.

Balis, D., P. Valks, and R. van Oss (2003), TOGOMI Delta Validation Document, Issue 1.0, TOGOMI/KNMI/VAL/001, KNMI/ESA, October 2003. Available at http://www.gse-promote.org/services/ozone_nrt/togomi_validation_v1.0.pdf

Balis, D., J. C. Lambert, M. Van Roozendael, R. Spurr, D. Loyola, Y. Livschitz, P. Valks, V. Amiridis, P. Gerard, J. Granville, and C. Zehner (2007a), Ten years of GOME/ERS2 total ozone data: the new GOME Data Processor (GDP) Version 4: II. Ground-based validation and comparisons with TOMS V7/V8, J. Geophys. Res., 112, D07307, doi:10.1029/2005JD006376.

Balis, D., M. Kroon, M. E. Koukouli, E. J. Brinksma, G. Labow, J. P. Veefkind, and R. D. McPeters (2007b), Validation of Ozone Monitoring Instrument total ozone column measurements using Brewer and Dobson spectrophotometer ground-based observations, J. Geophys. Res., 112, D24S46, doi:10.1029/2007JD008796.

Bracher, A., L. N. Lamsal, M. Weber, K. Bramstedt, M. Coldewey-Egbers, and J. P. Burrows (2005), Global satellite validation of SCIAMACHY O3 columns with GOME WFDOAS, Atmos. Chem. Phys., 5, 2357–2368.

Burrows, J. P., M. Weber, M. Buchwitz, V. Razonov, A. Ladstatter, A. Richter, R. De Beerk, R. Hoogen, D. Bramsdted, K.U. Eichmann, M. Eisenger, and D. Perner (1999), The Global Ozone Monitoring Experiment (GOME): mission concept and first scientific results, J. Atmos. Sci., 56, 151–175.

Bhartia, P. K., and C. Wellemeyer (2002), TOMS-V8 total O3 algorithm, in OMI Algorithm Theoretical Basis Document, vol. II, OMI Ozone Products, edited by P. K. Bhartia, pp. 15–31, NASA Goddard Space Flight Cent., Greenbelt, Md. Available at http://eospso.gsfc.nasa.gov/eos_homepage/for_scientists/atbd/index.php

Bojkov, R. D., L. Bishop, W. J. Hill, G. C. Reinsel, and G. C. Tiao (1990), A statistical trend analysis of revised Dobson total ozone data over the Northern Hemisphere, J. Geophys. Res., 95, 9785–9807.

Bovensmann, H., J. P. Burrows, M. Buchwitz, J. Frerick, S. Noel, V. V. Rozanov, K. V. Chance, and A.P.H. Goede (1999), SCIAMACHY: Mission objectives and measurement modes, J. Atmos. Sci., 56, 127–150.

Bramstedt, K., J. Gleason, D. Loyola, W. Thomas, A. Bracher, M. Weber, and J. P. Burrows (2003), Comparison of total ozone from the satellite instruments GOME and TOMS with measurements from the Dobson network 1996– 2000, Atmos. Chem. Phys., 3, 1409– 1419.

Callis, L. B., M. Natarajan, J. D. Lambeth, and R. E. Boughner (1997), On the origin of midlatitude ozone changes: Data analysis and simulations for 1979–1993, J. Geophys. Res., 102, 1215–1228.

Coldewey-Egbers, M., M. Weber, L. N. Lamsal, R. de Beek, M. Buchwitz, and J. P. Burrows (2005), Total ozone retrieval from GOME UV spectral data using the weighting function DOAS approach, Atmos. Chem. Phys., 5, 1015–1025.

De Haan, J. F., P. B. Bosma, and J. W. Hovenier (1987), The adding method for multiple scattering calculations of polarized light, Astron. Astrophys, 183, 371-391.

De Haan, J.F. (2003), Accounting for Raman Scattering in DOAS, Technical Report SN-OMIE-KNMI-409, KNMI, De Bilt, The Netherlands. Available at http://www.gse-promote.org/services/ozone_nrt/DeHaan_OMI_Raman_DOAS_v_1.pdf

Eskes, H. J., R. J. van der A, E. J. Brinksma, J. P. Veefkind, J. F. de Haan, and P. J. M. Valks (2005), Retrieval and validation of ozone columns derived from measurements of SCIAMACHY on ENVISAT, Atmos. Chem. Phys. Discuss., 5, 4429–4475.

Eskes, H. J., R. J. van der A, and E. J. Brinksma (2006), TOSOMI Algorithm Document. Technical Report TEM/AD3/002, Issue 1.0, 09/08/2006, KNMI, De Bilt, The Netherlands. Available at http://www.temis.nl/docs/AD_TOSOMI.pdf

Fioletov, V. E., J. B. Kerr, D. I. Wardle, N. Krotkov, and J. R. Herman (2002), Comparison of Brewer ultraviolet irradiance measurements with total ozone mapping spectrometer satellite retrievals, Opt. Eng., 41, 3051–3061.

Fioletov, V. E., J. B. Kerr, C. T. McElroy, D. I. Wardle, V. Savastiouk, and T. S. Grajnar (2005), The Brewer reference triad, Geophys. Res. Lett., 32, L20805, doi:10.1029/2005GL0242442.

Farman, J. C., B. G. Gardiner, and J. D. Shanklin (1985), Large losses of total ozone in Antarctica reveal seasonal ClOx/NOx interaction, Nature, 315, doi:10.1038/315207a0.

Fusco, A. C., and M. L. Salby (1999), Interannual variations of total ozone and their relationship to variations of planetary wave activity, J. Clim., 12, 1619–1629.

Gurlit, W., H. Bösch, H. Bovensmann, J.P. Burrows, A. Butz, C. Camy-Peyret, M. Dorf, K. Gerilowski, A. Lindner, S. Nöel, U. Platt, F. Weidner, and K. Pfeilsticker (2005), The UV-A and visible solar irradiance spectrum: inter-comparison of absolutely calibrated, spectrally medium resolution solar irradiance spectra from balloon- and satellite-borne measurements, Atmos. Chem. Phys., 5, 1879–1890.

Hadjinicolaou, P., A. Jrrar, J. A. Pyle, and L. Bishop (2002), The dynamically driven long-term trend in stratospheric ozone over northern middle latitudes, Q. J. R. M. S., 128, 1393– 1412.

Harris, N. R. P., J. Ancellet, L. Bishop, D.J. Hofmann, J. B. Kerr, R. D. McPeters, M. Prendez, W. J. Randell, J. Staehelin, R. H. Subkharaya, A. Volz-Thomas, J. Zawodny, and C. Zerefos (1997), Trends in stratospheric and free tropospheric ozone, J. Geophys. Res., 102, 1571–1590.

Hood, L. L., J. P. McCormack, and K. Labitzke (1997), An investigation of dynamical contributions to midlatitude ozone trends in winter, J. Geophys. Res., 102, 13079–13093.

Kerr, J. B. (2002), New methodology for deriving total ozone and other atmospheric variables from Brewer spectrophotometer direct sun spectra, J. Geophys. Res., 107(D23), 4731, doi:10.1029/2001JD001227.

Kiehl, J. T., T. L. Schneider, R. W. Portmann, and S. Solomon (1999), Climate forcing due to tropospheric and stratospheric ozone, J. Geophys. Res., 104, 31239–31254.

Koelemeijer, R. B. A, and P. Stammes (1999), Effects of clouds on ozone column retrieval from GOME UV measurements, J. Geophys. Res., 104, 8281–8294.

Lerot, C., M. Van Roozendael, J. van Geffen, J. van Gent, C. Fayt, R. Spurr, G. Lichtenberg, and A. von Bargen, (2009) Six years of total ozone column measurements from SCIAMACHY nadir observations, Atmos. Meas. Tech., 2, 87–98.

Levelt, P. F., E. Hilsenrath, G. W. Leppelmeier, G. H. J. Van den Oord, P. K. Bhartia, J. Tamminen, J. F. De Haan, and J. P. Veefkind (2006), The Ozone Monitoring Instrument, IEEE Trans. Geosci. Remote Sens., 44(5), 1093– 1101, doi:10.1109/TGRS.2006.872333.

Loyola, D., M. E. Koukouli, P. Valks, D. S. Balis, N. Hao, M. Van Roozendael, R. J. D. Spurr, W. Zimmer, S. Kiemle, C. Lerot, and J-C. Lambert (2011), The GOME-2 Total Column Ozone Product: Retrieval Algorithm and Ground-Based Validation, J. Geophys. Res., 116, D07302, doi:10.1029/2010JD014675.

Marquard, L. C., T. Wagner, and U. Platt (2000), Improved air mass factor concepts for scattered radiation differential optical absorption spectroscopy of atmospheric species, J. Geophys. Res., 105, 1315.

McPeters, R. D., P. K. Bhartia, A. J. Krueger, and J. R. Herman (1998), Earth Probe Total Ozone Mapping Spectrometer (TOMS) Data Products User’s Guide. NASA Reference Publication. NASA, Greenbelt, MD.

Molina, M. J. and F.S. Rowland (1974), Stratospheric sink for chlorofluoromethanes: Chlorine atom-catalyzed destruction of ozone, Nature, 249, 810–812.

Munro, R., M. Eisinger, C. Anderson, J. Callies, E. Corpaccioli, R. Lang, A. Lefebvre, Y. Livschitz, and A. Perez Albinana (2006), GOME-2 on METOP: From in-orbit verification to routine operations, in: Proceedings of EUMETSAT Meteorological Satellite Conference, Helsinki, Finland.

Platt, U. (1994), Differential optical absorption spectroscopy (DOAS), in Air Monitoring by

Spectroscopic Techniques, Chem. Anal. Ser., vol. 127, edited by W. Sigrist, pp. 22–85, John Wiley, New York.

Platt, U. (1999), Modern methods of the measurements of atmospheric trace gases, Phys. Chem. Phys., 1, 5409–5415.

Popp, C., P. Wang, D. Brunner, P. Stammes, Y. Zhou, and M. Grzegorski (2011), MERIS albedo climatology for FRESCO+ O2 A-band cloud retrieval, Atmos. Meas. Tech., 4, 463-483, doi:10.5194/amt-4-463-2011.

Redondas, A., E. Cuevas, and A. Labajo (2002), Management and QA/QC of the Spanish Brewer spectrophotometer network, in Sixth European Symposium on Stratospheric Ozone [CD-ROM], edited by N. R. P. Harris, G. T. Amanatidis, and J. G. Levine, Comm. of the Eur. Commun., Goteborg, Sweden.

Redondas, A., and A. Cede (2006), Brewer algorithm sensitivity analysis, paper presented at the SAUNA workshop, Puerto de la Cruz, Tenerife, November, 2006.

Redondas, A., et al. (2008), Second intercomparison campaign of the Regional Brewer Calibration Center-Europe, paper presented at the Quadrennial Ozone Symposium, Eur. Comm., Tromso, Norway.

Rex, M., R. J. Salawitch, P. von der Gathen, N. R. P. Harris, M. Chipperfield, and B. Naujokat (2004), Arctic ozone loss and climate change, Geophys. Res. Lett., 31, L04116, doi:10.1029/2003GL018844.

Skupin, J., S. Nöel, M.W. Wuttke, M. Gottwald, H. Bovensmann, M. Weber, and J.P. Burrows (2005), SCIAMACHY Solar Irradiance Observation in the Spectral Range from 240 to 2380 nm, Adv. Space Res., 35, 370–375.

Solomon, S., A. L. Schmeltekopf, and R. W. Saunders (1987), On the interpretation of zenith-sky absorption measurements, J. Geophys. Res., 92, 8311–8319.

Solomon, S. (1999), Stratospheric ozone depletion: A review of concepts and history, Rev. Geophys., 37(3), 275– 316.

Staehelin, J., N. R .P. Harris, C. Appenzeller, J. Bernhard, and M. Piechowski (2001), Observations of ozone trends, Rev. Geophys., 39, 231–290.

Steinbrecht, W., H. Claude, U. Köhler, and K. P. Hoinka (1998), Correlations between tropopause height and total ozone: Implications for long-term changes, J. Geophys. Res., 103, 19183-19192.

Stolarski, R. S., A. J. Krueger, M. R. Schoeberl, R. D. McPeters, P. A. Newman, and J. C. Alpert (1986), Nimbus 7 satellite measurements of the springtime Antarctic ozone decrease, Nature, 322, 808–811.

Stolarski, R., R. Bojkov, L. Bishop, C. Zerefos, J. Staehelin, and J. Zawodny (1992), Measured trends in stratospheric ozone, Science, 256, 342– 349.

Tilstra, L. G., and P. Stammes (2005), Alternative polarization retrieval for SCIAMACHY in the ultraviolet, Atmos. Chem. Phys., 5, 2099–2107.

Valks, P., and R. van Oss (2003), TOGOMI Algorithm Theoretical Basis Document, Issue 1.2, TOGOMI/KNMI/ATBD/001, KNMI/ESA, November 2003. Available at http://www.gse-promote.org/services/ozone_nrt/togomi_ATBD_v1.21.pdf

van Oss, R., P. Valks and J. de Haan (2004), TOGOMI Delta Validation Document, Issue 1.0, TOGOMI/KNMI/VAL/002, KNMI/ESA, January 2004. Available at http://www.gse-promote.org/services/ozone_nrt/togomi_deltavalidation_v1.0.pdf

van Roozendael, M., D. Loyola, R. Spurr, D. Balis, J.C. Lambert, Y. Livschitz, P. Valks, T. Ruppert, P. Kenter, C. Fayt, and C. Zehner (2006), Ten years of GOME/ERS-2 total ozone data – The new GOME data processor (GDP) version 4: 1. Algorithm description, J. Geophys. Res., 111, D14311, doi:10.1029/2005JD006375.

Veefkind, J. P., J. F. de Haan, E. J. Brinksma, M. Kroon, and P. F. Levelt (2006), Total Ozone from the Ozone Monitoring Instrument (OMI) using the DOAS technique, IEEE Trans. Geosci. Remote Sens., 44, 1239–1244, doi:10.1109/TGRS.2006.871204.

Wang, P., Stammes, P., R. van der A, G. Pinardi, and M. van Roozendael (2008), FRESCO+: an improved O2 A-band cloud retrieval algorithm for tropospheric trace gas retrievals, Atmos. Chem. Phys., 8, 6565–6576.

World Meteorological Organization (WMO) (1996), Guide to meteorological instruments and methods of observation, 6th ed., WMO Publication #8, Geneva, Switzerland.

World Meteorological Organization (WMO) (2010), Scientific assessment of ozone depletion: Global ozone research and monitoring project, Tech. Rep. 52, Geneva, Switzerland.

FIGURES LEGENDS

Figure 1. Locations of the five Brewer spectrophotometers at the Iberian Peninsula: A Coruña (43.33ºN, 8.42ºW), Zaragoza (41.01ºN, 1.01ºW), Madrid (40.45ºN, 3.72ºW), Murcia (38.03ºN, 1.17ºW) and El Arenosillo (37.06ºN, 6.44ºW).

Figure 2. Correlation between satellite and ground-based TOC data gathered over the Iberian Peninsula during six consecutive years (2004–2009). (top) SCIAMACHY versus Brewer and (bottom) GOME versus Brewer. The solid line represents the unit slope to with which the data almost agree.

Figure 3. Time series of the daily relative difference between satellite (top, SCIAMACHY; bottom, GOME) and ground-based TOC data gathered over the Iberian Peninsula during six consecutive years (2004–2009). Here a running mean over ten days was applied.

Figure 4. Differences between TOC data retrieved by satellite (top, SCIAMACHY; bottom, GOME) and ground-based Brewer as function of satellite solar zenith angle for all, cloud-free, broken-cloud, and fully clouded conditions.

Figure 5. Differences between TOC data retrieved by satellite (top, SCIAMACHY; bottom, GOME) and ground-based Brewer as function of satellite viewing zenith angle for all, cloud-free, broken-cloud, and fully clouded conditions.

Figure 6. Differences between TOC data retrieved by satellite (top, SCIAMACHY; bottom, GOME) and ground-based Brewer as function of satellite cloud fraction for all, low and high solar zenith angles.

Figure 7. Differences between TOC data retrieved by satellite (top, SCIAMACHY; bottom, GOME) and ground-based Brewer as function of satellite cloud top pressure for all, low and high solar zenith angles.

Figure 8. Differences between TOC data retrieved by satellite (SCIAMACHY, top; GOME, bottom) and ground-based Brewer as function of ground-based TOC data for all, low and high solar zenith angles.

TABLES AND THEIR LEGENDS

Table 1. Parameters obtained in the correlation analysis between SCIAMACHY TOC data (upper rows) and Brewer measurements as gathered over the Iberian Peninsula during the period 2004-2009. Results for the GOME correlation are shown in the lower rows. The parameters are the following: the number of data (N), the slope of the regression, the correlation coefficients (R^2), the root-mean-square errors (RMSE), the mean bias (MB) and the mean absolute bias (MAB).

	N	**Slope**	**R^2**	**RMSE (%)**	**MB (%)**	**MAB (%)**
Madrid	407	1.00±0.01	0.96	2.29	-0.90±2.26	1.76±1.68
	497	1.02±0.01	0.96	2.31	-0.76±2.29	1.78±1.63
Murcia	633	0.99±0.01	0.95	2.23	-2.09±2.18	2.52±1.67
	847	1.00±0.01	0.94	2.42	-1.45±2.39	2.14±1.79
Coruña	555	1.01±0.01	0.96	2.36	-1.41±2.32	2.12±1.70
	787	0.99±0.01	0.95	2.48	-1.56±2.45	2.23±1.87
Zaragoza	558	1.00±0.01	0.96	2.23	-0.98±2.20	1.85±1.55
	773	1.00±0.01	0.96	2.15	-0.93±2.13	1.75±1.52
Arenosillo	570	0.98±0.01	0.96	1.99	-0.70±1.98	1.57±1.39
	748	1.00±0.01	0.95	2.00	-0.51±1.98	1.49±1.40
Iberian Peninsula	2723	1.00±0.01	0.95	2.28	-1.26±2.25	1.99±1.63
	3652	1.00±0.01	0.95	2.32	-1.08±2.29	1.90±1.68


Coruña
Zaragoza
Madrid
Murcia
Arenosillo

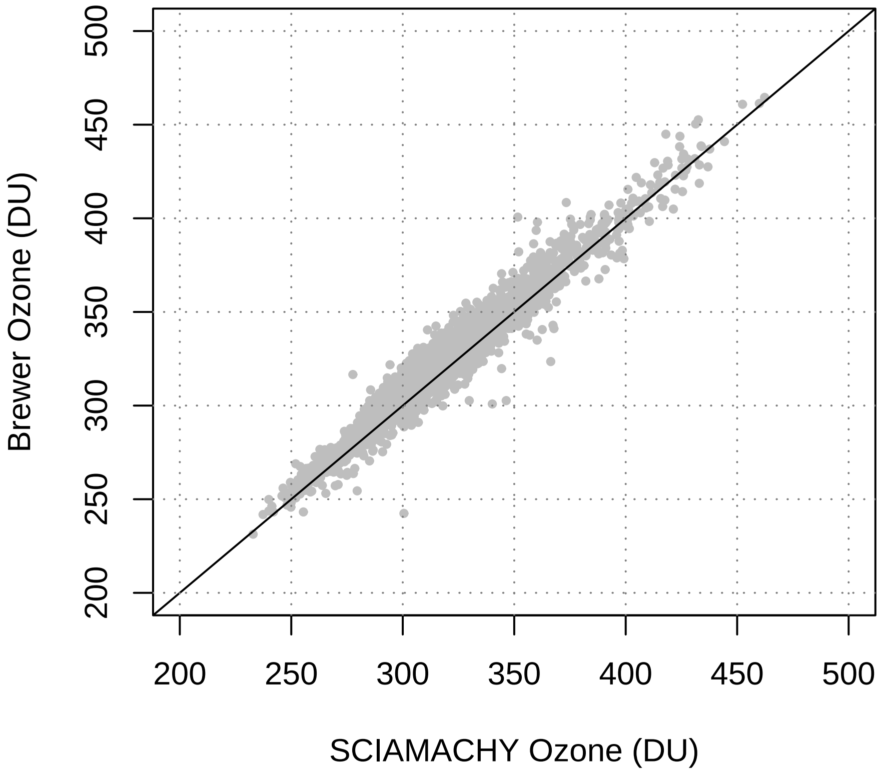
Brewer Ozone (DU)
200
250
300
350
400
450
500
SCIAMACHY Ozone (DU)

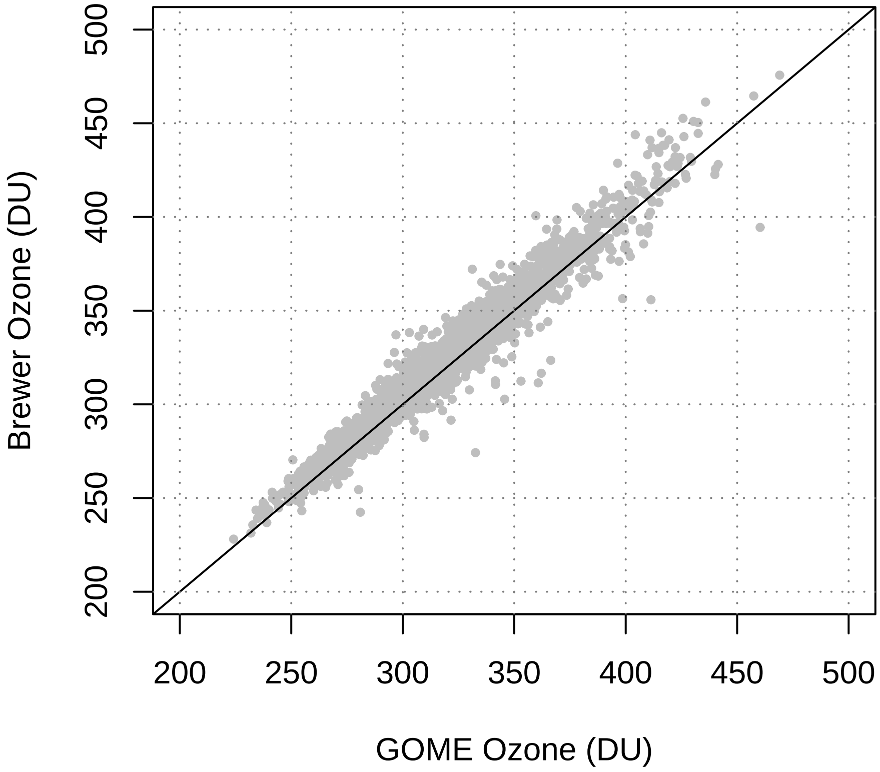
Brewer Ozone (DU)
200
250
300
350
400
450
500
GOME Ozone (DU)

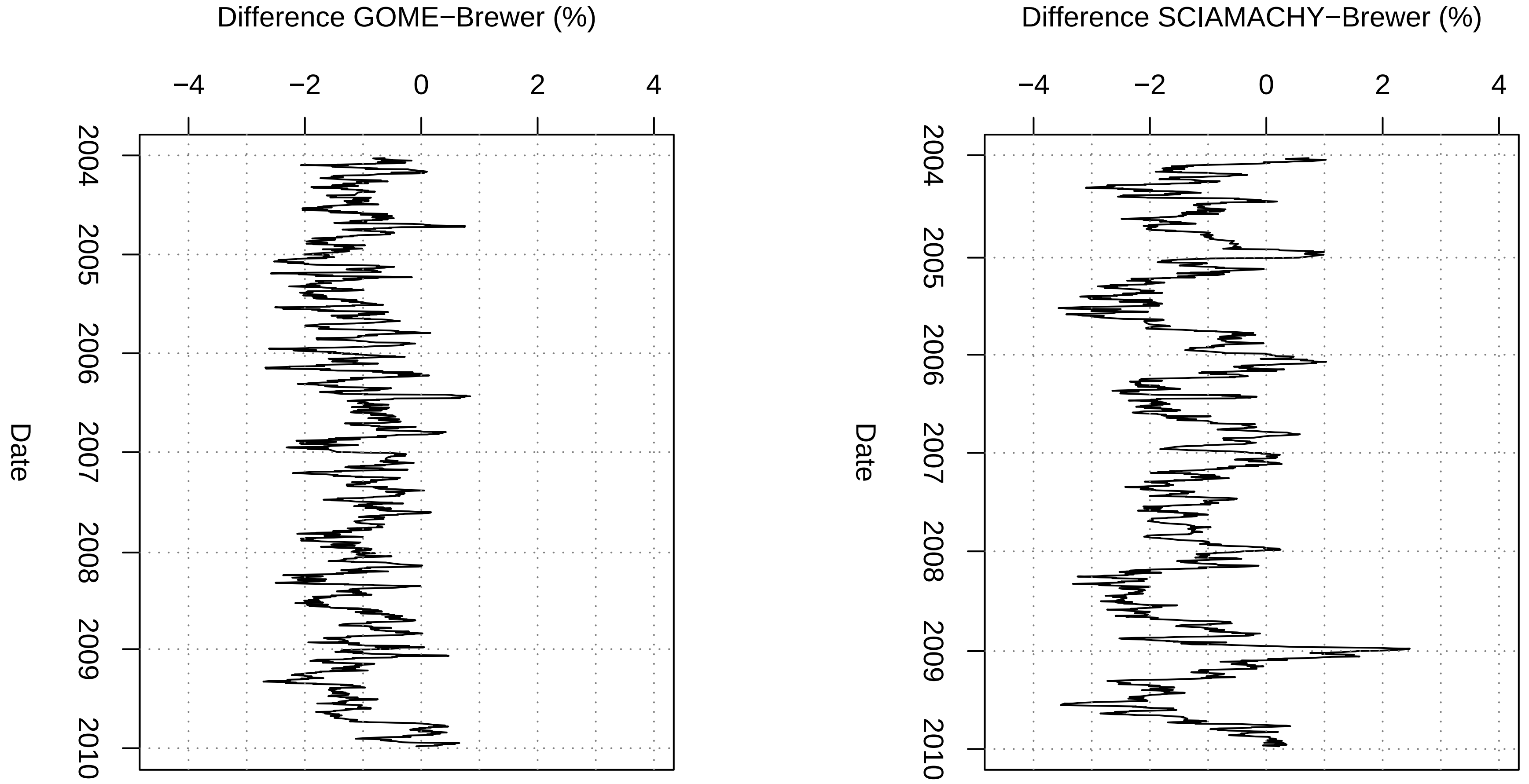

Difference GOME−Brewer (%)
−4
−2
0
2
4
2004
2005
2006
2007
2008
2009
2010
Date
Difference SCIAMACHY−Brewer (%)
−4
−2
0
2
4
2004
2005
2006
2007
2008
2009
2010
Date

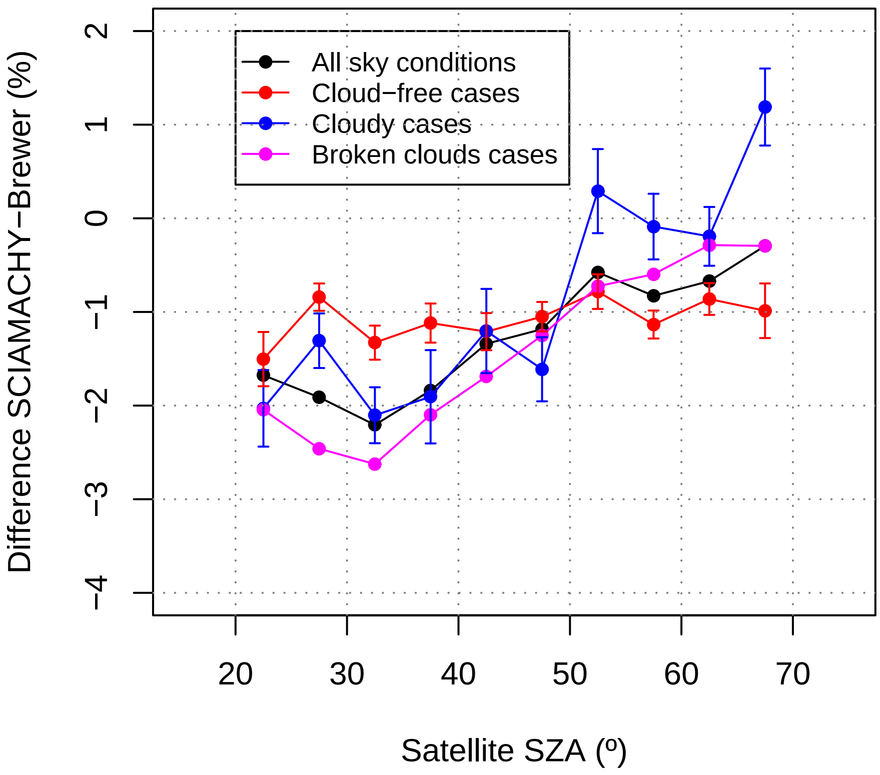

All sky conditions
Cloud−free cases
Cloudy cases
Broken clouds cases
Difference SCIAMACHY−Brewer (%)
2
1
0
−1
−2
−3
−4
20
30
40
50
60
70
Satellite SZA (º)

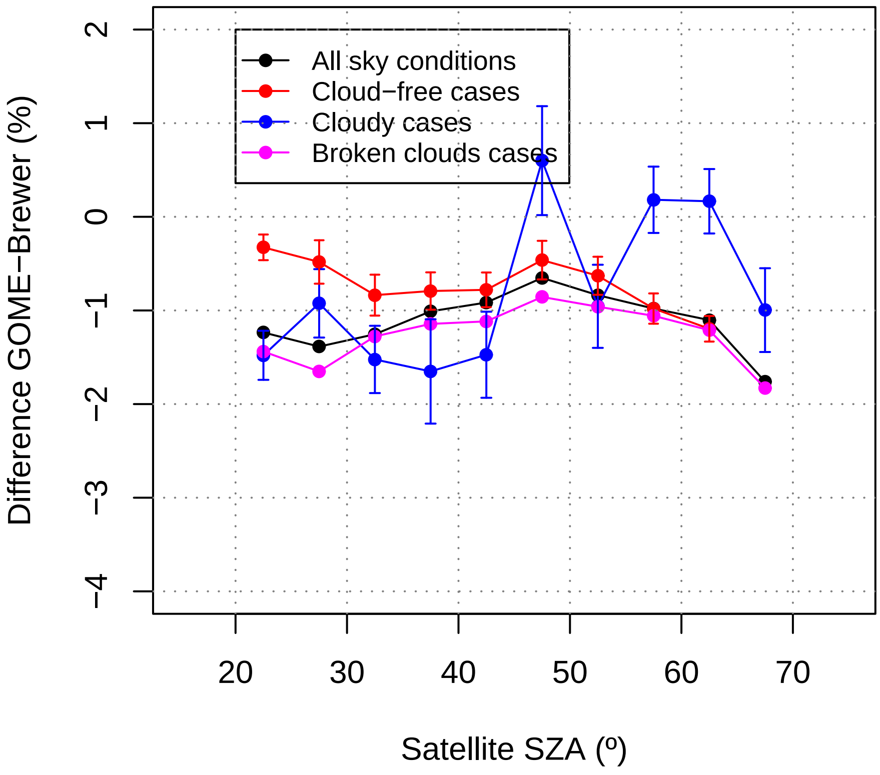

All sky conditions
Cloud−free cases
Cloudy cases
Broken clouds cases
Difference GOME−Brewer (%)
2
1
0
−1
−2
−3
−4
20
30
40
50
60
70
Satellite SZA (º)

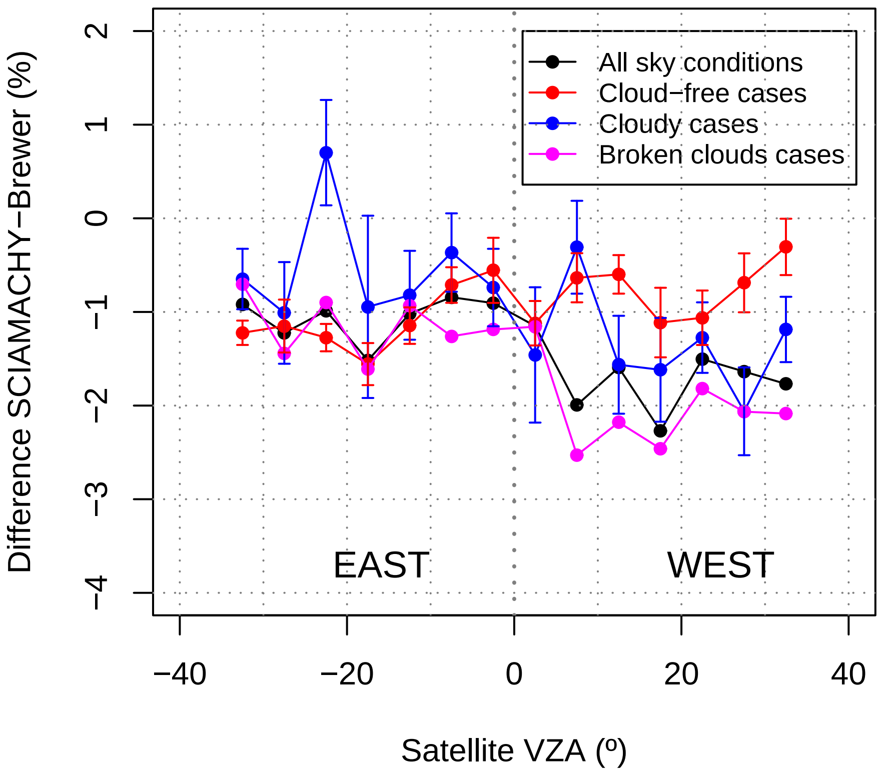
All sky conditions
Cloud−free cases
Cloudy cases
Broken clouds cases
EAST
WEST
Difference SCIAMACHY−Brewer (%)
Satellite VZA (º)
−40
−20
0
20
40
2
1
0
−1
−2
−3
−4

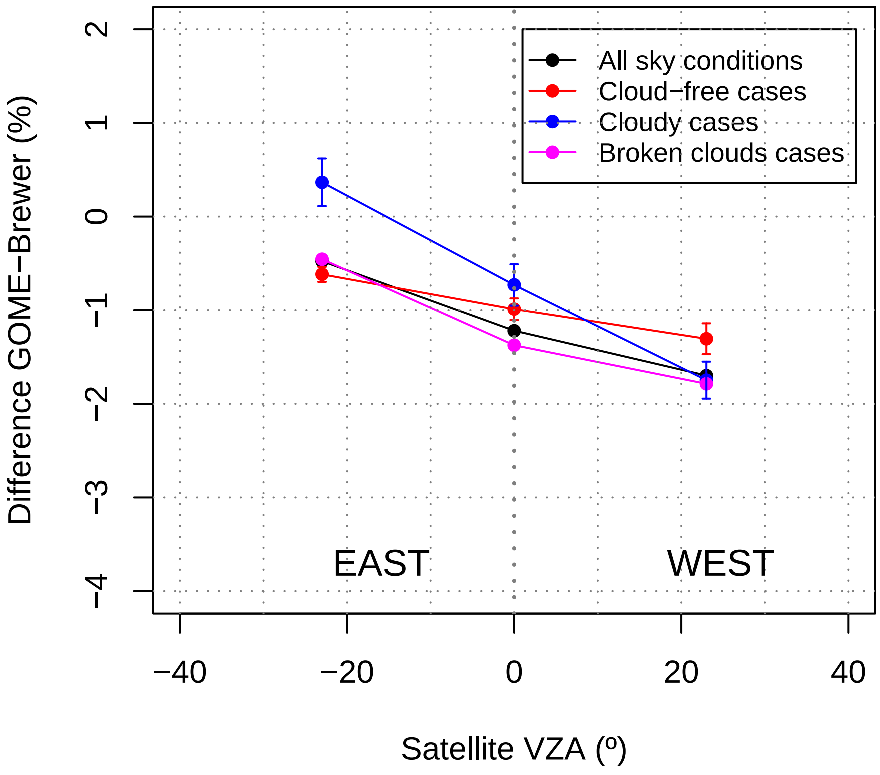
All sky conditions
Cloud−free cases
Cloudy cases
Broken clouds cases
EAST
WEST
Difference GOME−Brewer (%)
Satellite VZA (º)
−40
−20
0
20
40
2
1
0
−1
−2
−3
−4

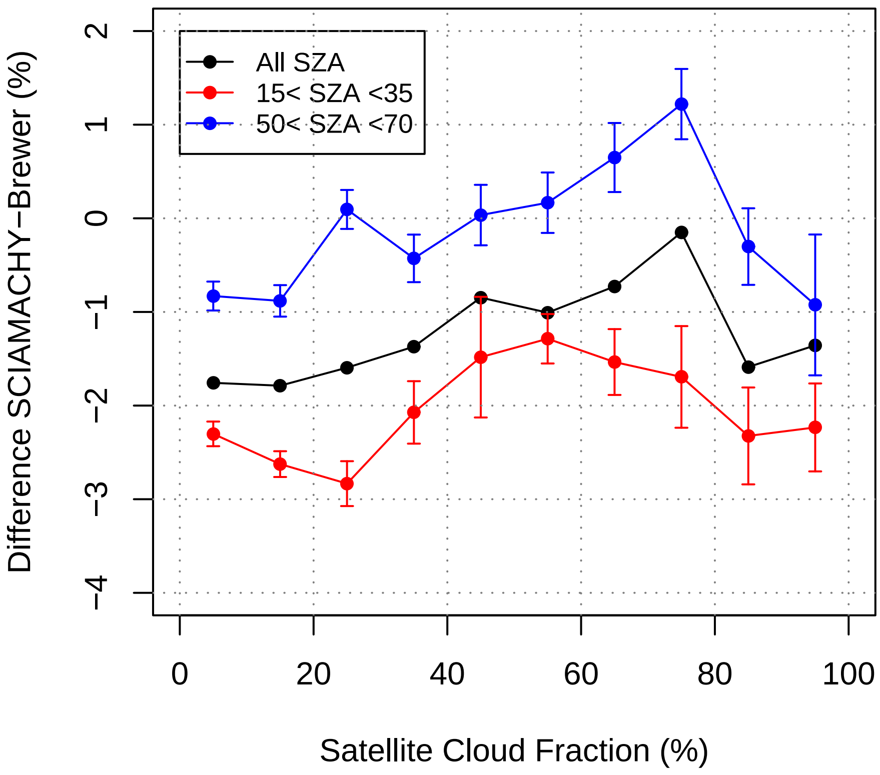
All SZA
15< SZA <35
50< SZA <70
Difference SCIAMACHY−Brewer (%)
Satellite Cloud Fraction (%)

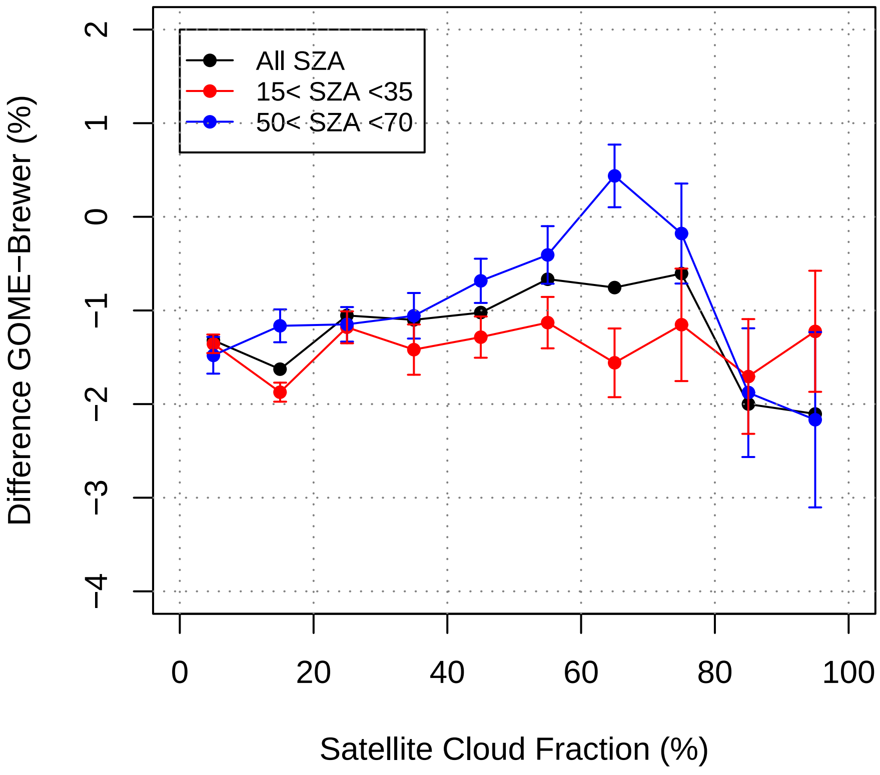
All SZA
15< SZA <35
50< SZA <70
Difference GOME−Brewer (%)
Satellite Cloud Fraction (%)

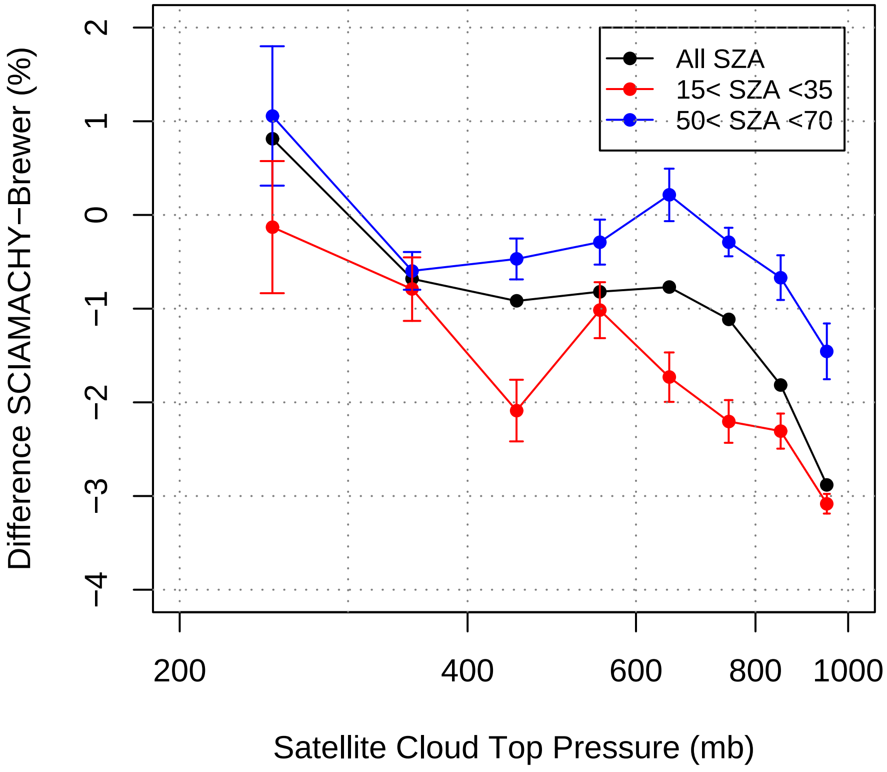
All SZA
15< SZA <35
50< SZA <70
Difference SCIAMACHY−Brewer (%)
2
1
0
−1
−2
−3
−4
200
400
600
800
1000
Satellite Cloud Top Pressure (mb)

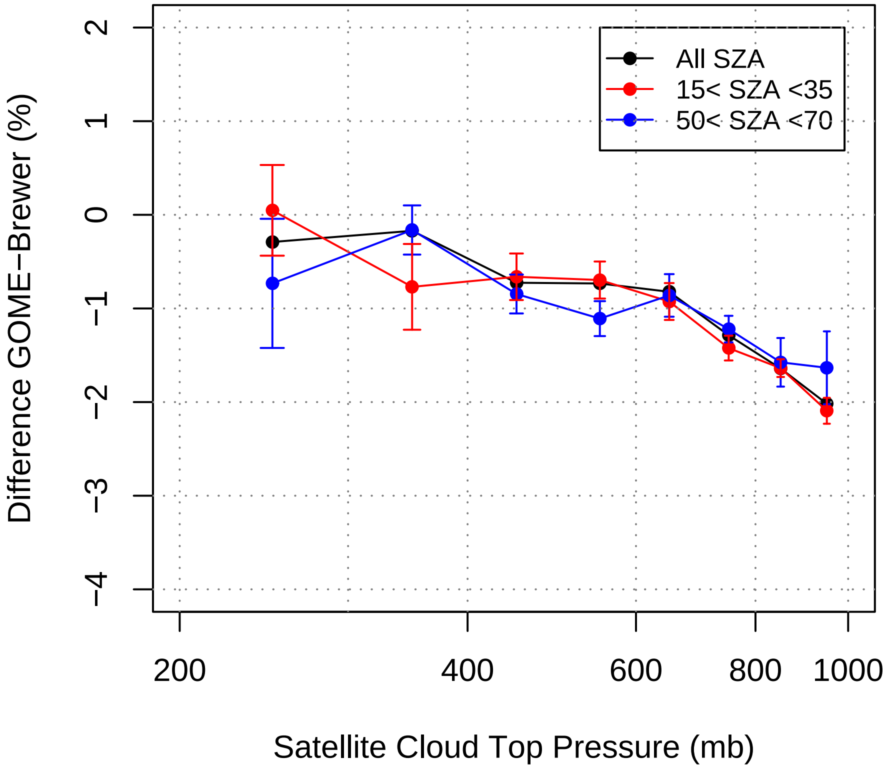
All SZA
15< SZA <35
50< SZA <70
Difference GOME−Brewer (%)
2
1
0
−1
−2
−3
−4
200
400
600
800
1000
Satellite Cloud Top Pressure (mb)

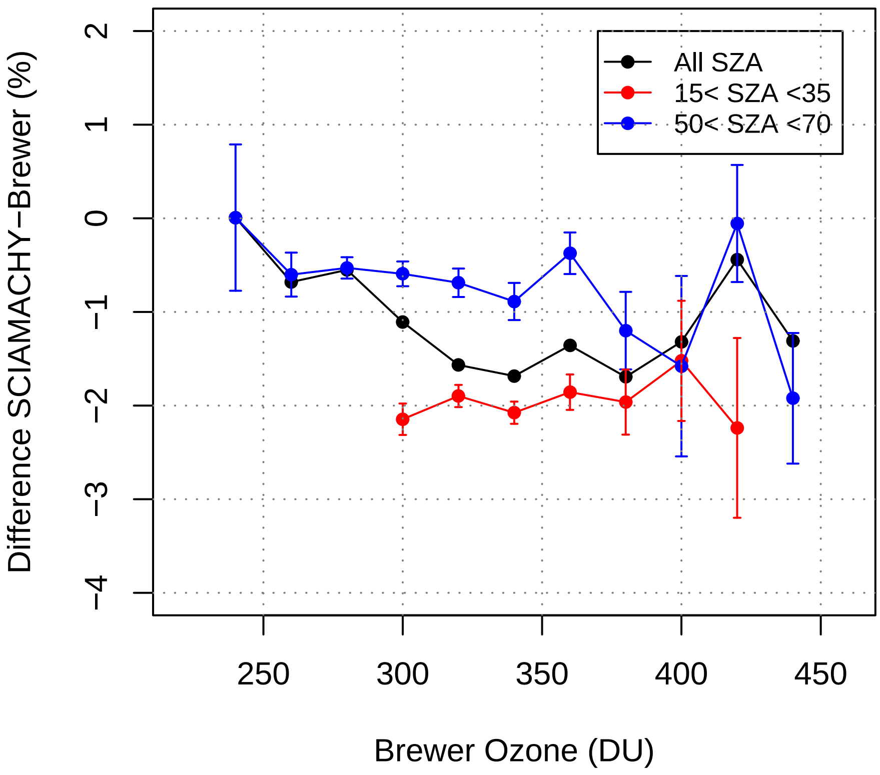

All SZA
15< SZA <35
50< SZA <70
Difference SCIAMACHY−Brewer (%)
Brewer Ozone (DU)

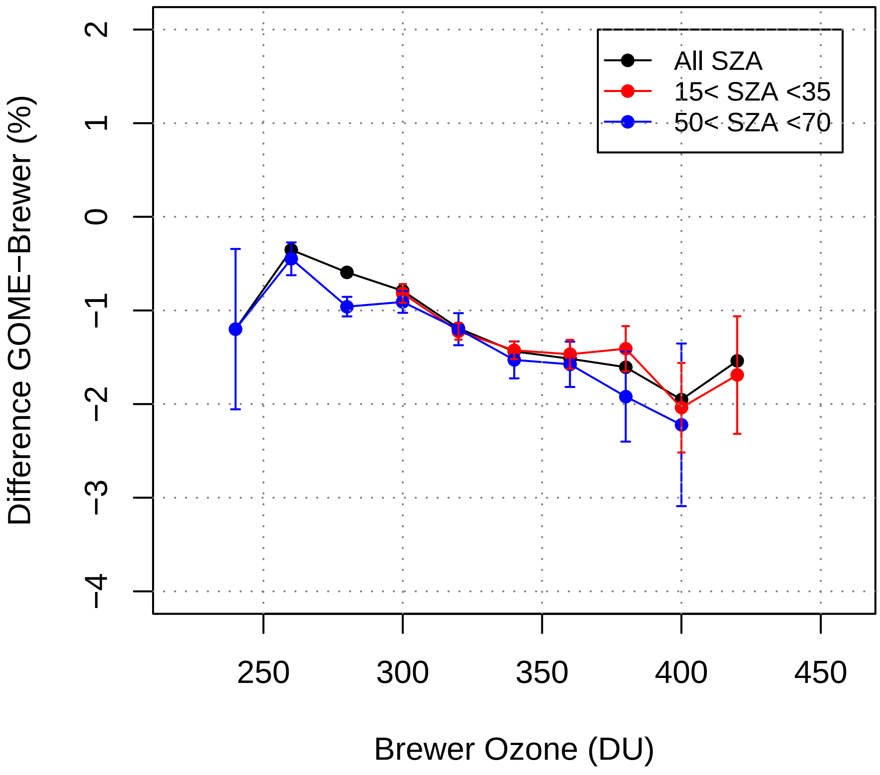

All SZA
15< SZA <35
50< SZA <70
Difference GOME−Brewer (%)
Brewer Ozone (DU)